Apolipoprotein E Is the Major Physiological Activator of Lecithin−Cholesterol Acyltransferase (LCAT) on Apolipoprotein B Lipoproteins†

Yue Zhao,‡ Fayanne E. Thorngate,§ Karl H. Weisgraber,|| David L. Williams,§,⊥ and John S. Parks*,‡

Department of Pathology, Wake Forest University School of Medicine, Medical Center Boulevard, Winston-Salem, North Carolina 27157, Department of Pharmacological Sciences, University Medical Center, State University of New York, Stony Brook, New York 11794, and Gladstone Institute of Cardiovascular Disease and the Department of Pathology, University of California, San Francisco, California 94141

Received August 26, 2004; Revised Manuscript Received October 13, 2004

ABSTRACT: Our previous studies have indicated that lecithin−cholesterol acyltransferase (LCAT) contributes significantly to the apoB lipoprotein cholesteryl ester (CE) pool. Cholesterol esterification rate (CER) in *apoA-I*$^{-/-}$ *apoE*$^{-/-}$ mouse plasma was <7% that of C57Bl/6 (B6) mouse plasma, even though *apoA-I*$^{-/-}$ *apoE*$^{-/-}$ plasma retained $^1/_3$ the amount of B6 LCAT activity. This suggested that lack of LCAT enzyme did not explain the low CER in *apoA-I*$^{-/-}$ *apoE*$^{-/-}$ mice and indicated that apoE and apoA-I are the only major activators of LCAT in mouse plasma. Deleting apoE on low-density lipoprotein (LDL) reduced CER (1% free cholesterol (FC) esterified/h) compared to B6 (6% FC esterified/h) and *apoA-I*$^{-/-}$ (11% FC esterified/h) LDL. Similar sized LDL particles from all four genotypes were isolated by fast protein liquid chromatography (FPLC) after radiolabeling with [^{3}H]-free cholesterol (FC). LDLs (1 μg FC) from each genotype were incubated with purified recombinant mouse LCAT; LDL particles from B6 and *apoA-I*$^{-/-}$ plasma were much better substrates for CE formation (5.7% and 6.3% CE formed/30 min, respectively) than those from *apoE*$^{-/-}$ and *apoE*$^{-/-}$ *apoA-I*$^{-/-}$ plasma (1.2% and 1.1% CE formed/30 min). Western blot analysis showed that the amount of apoA-I on *apoE*$^{-/-}$ LDLs was higher compared to B6 LDL. Adding apoE to incubations of *apoA-I*$^{-/-}$ *apoE*$^{-/-}$ very low density lipoprotein (VLDL) resulted in a 3-fold increase in LCAT CER, whereas addition of apoA-I resulted in a more modest 80% increase. We conclude that apoE is a more significant activator of LCAT than apoA-I on mouse apoB lipoproteins.

Cholesterol esters (CEs)[1] in plasma are derived from two sources, the intracellular enzyme acyl CoA−cholesterol acyltransferase (ACAT) and the plasma enzyme lecithin−cholesterol acyltransferase (LCAT). ACAT uses free cholesterol (FC) and fatty acyl-CoAs as substrates for CE synthesis (*1*, *2*). In liver and intestine, ACAT-derived CEs enter the plasma compartment via secretion of triglyceride (TG)-rich lipoproteins (LPs), such as chylomicrons and very low density lipoproteins (VLDL). Plasma VLDLs are metabolized to LDL, which are CE-enriched particles with a prolonged residence time in plasma. LCAT (EC 2.3.1.43) is a 65-kDa glycoprotein that is synthesized predominantly in the liver and secreted into plasma, where it catalyzes the conversion of FC to CE on the surface of lipoproteins (*3*). The LCAT reaction involves two steps, the hydrolysis (i.e., phospholipase A_2 activity) of an sn-2 fatty acid from phospholipid (PL), followed by the transacylation of the fatty acyl group to the 3β-hydroxyl group of cholesterol to generate CE and lysolecithin (*4*). Because the sn-2 position of phospholipids is more enriched in polyunsaturated fatty acids, LCAT-derived CEs are relatively enriched in polyunsaturated fatty acyl species (*5*, *6*).

The preferred lipoprotein substrate of LCAT is high-density lipoprotein (HDL), which contains the main apolipoprotein activator of LCAT, apoA-I (*7*). LCAT is important in the maturation of nascent HDL particles, lacking a neutral lipid core, into mature spherical HDL particles that contain a core of CEs. Whereas LCAT primarily associates with HDL in plasma (*8*, *9*), the enzyme has also been shown to be active in the LDL fraction (*8*−*11*). In human plasma, 33% of the newly synthesized CE was found in the LDL fraction and, in human plasma devoid of cholesteryl ester transfer protein (CETP) activity, 25% of newly synthesized CE was generated in LDL particles (*11*). These data demonstrate that LCAT is a quantitatively important source of LDL CE in human plasma even in the absence of CETP. Thus, LCAT exhibits two activities in normal plasma: α-LCAT activity, specific for lipoproteins that migrate with α-mobility on agarose gel electrophoresis (i.e., HDL) and β-LCAT activity, which is specific for pre-β and β-migrating lipoproteins (i.e., VLDL and LDL) (*12*). The rate of reaction on apoB LPs is slow compared to that on HDL (*12*, *13*).

† This work was supported by National Institutes of Health Grants HL-54176 (JSP), HL-49373 (JSP), HL-32868 (DLW), and American Heart Association grants 0215153U (YZ).

* To whom correspondence should be addressed: tel, 336-716-2145; fax, 336-716-6279; e-mail, jparks@wfubmc.edu.

‡ Wake Forest University School of Medicine.

§ State University of New York, Stony Brook.

|| University of California, San Francisco.

⊥ Deceased.

[1] Abbreviations: CE, cholesteryl ester; CER, cholesterol esterification rate; B6, C57Bl/6; FC, free cholesterol; LCAT, lecithin−cholesterol acyltransferase; ACAT, acyl CoA−cholesterol acyltransferase; FER, fractional esterification rate; PL, phospholipid; TG, triglyceride; MER, molar esterification rate; LP, lipoprotein; HDL, high-density lipoprotein; LDL, low-density lipoprotein; VLDL, very low density lipoprotein.

10.1021/bi0481489 CCC: $30.25
Published on Web 12/29/2004

In humans, mutations in the LCAT gene are associated with complete absence of plasma LCAT activity, leading to familial LCAT deficiency (FLD), whereas the loss of α-LCAT activity on HDL results in fish eye disease (FED). Both FLD and FED lead to HDL deficiency, characterized by decreased CE-enriched mature α-HDL and increased FC-enriched small spherical HDL or disk-shaped pre-β HDL (*14*−*16*). In addition, patients with FLD have VLDL/LDL particles that are abnormal in size and shape with large irregular multilamellar particles resembling sheets of bilayer membranes and LpX-like particles (*16*, *17*).[2] However, FED patients have normal β-LCAT activity and apoB lipoprotein particles in plasma that are normal in size and shape. These combined data suggest that LCAT not only is responsible for the maturation of nascent discoidal HDL (*18*) but may play a role in correcting the resulting imbalance between surface to core lipid that occurs during lipolysis of TG in apoB LPs. LCAT may directly function to remove excess surface PL and FC from apoB LP particles during lipolysis and subsequently used these lipid substrates for cholesterol esterification to generate mature HDL particles. Alternatively, LCAT may regenerate core lipid for apoB LPs by generating CE that replaces the TG lost during lipolysis. In either case, LCAT would be critical in the maintenance of normal LP size and shape.

To better understand the contribution of plasma LCAT in the in vivo generation of CE in apoB LPs, we crossed *LCAT*$^{-/-}$ mice into the *LDLr*$^{-/-}$ and *apoE*$^{-/-}$ backgrounds to retard the clearance and elevate plasma concentrations of apoB LPs (*19*). In apoB LPs, there was a 40% reduction in cholesteryl linoleate and a complete absence of CE species containing long chain (>18 carbon) polyunsaturated fatty acids (20:4, 20:5 n-3 and 22:6 n-3), from 29.3% to 0%, in *LDLr*$^{-/-}$ *LCAT*$^{-/-}$ compared to *LDLr*$^{-/-}$ mice with active LCAT, suggesting that LCAT was critical in the synthesis of these species. In a more recent study, a similar percentage composition of FC and CE was found in plasma LDLs of *LDLr*$^{-/-}$ and *ACAT2*$^{-/-}$ *LDLr*$^{-/-}$ mice, both containing active LCAT; however, plasma LDLs of *LCAT*$^{-/-}$ *LDLr*$^{-/-}$ mice had a reduced percentage of CE and increased percentage of FC (*41*). These data taken together indicated that LCAT makes a significant contribution to the in vivo generation of CE in apoB LPs and is responsible for the synthesis of nearly all long chain polyunsaturated CE fatty acid species.

It is well-known that the activity of LCAT depends on the presence of an apolipoprotein activator. The best activator of LCAT on recombinant HDL particles, which mimic nascent HDL in size and composition and on vesicles, is apoA-I, although most water-soluble apolipoproteins will activate LCAT, albeit to a lesser degree (*7*, *20*). Cheung et al. (*21*) demonstrated that LCAT-mediated cholesterol esterification occurred in human plasma devoid of apoA-I, after removal of apoA-I by immunoaffinity chromatography, and we showed that LCAT activity remained in the plasma of apoA-I knockout mice (*22*), indicating that other physiological activators of LCAT were present in plasma. ApoE exhibited about 20% of the activation potential of apoA-I on recombinant HDL particles (*20*, *23*) and has been found in association with distinct subfractions of LDL (*24*, *25*). However, there is no information regarding the role of apolipoproteins on LCAT activation of apoB LPs.

Our previous study raised the possibility that apoE might be a physiological activator of LCAT on apoB lipoproteins, because fewer LCAT-derived long chain polyunsaturated CEs were found in the apoB LP fraction of the *apoE*$^{-/-}$ mice compared to *LDLr*$^{-/-}$ mice, even though the activity of LCAT in plasma and the PL fatty acid composition was similar between the two genotypes of mice (*19*). In the present study, we had two goals: (1) to determine whether apoA-I and apoE were the only apolipoproteins involved in LCAT activation in plasma and (2) to determine whether apoE compared to apoA-I was more important in enzyme activation on apoB lipoproteins. Using in vivo and in vitro studies, we found that apoE and apoA-I are the only major physiological activators of LCAT in mouse plasma. In addition, our results suggested that apoE is a more significant physiological activator of LCAT than apoA-I on apoB LPs.

EXPERIMENTAL PROCEDURES

Experimental Animals and Animal Handing. B6, *apoA-I*$^{-/-}$ (B6 background), and *apoE*$^{-/-}$ (B6 background) mice were purchased from Jackson Labs (Bar Harbor, ME). The *apoA-I*$^{-/-}$ *apoE*$^{-/-}$ mice were created in a two-step breeding process. In the first step, *apoA-I*$^{-/-}$ mice were crossed with *apoE*$^{-/-}$ mice to generate *apoA-I*$^{+/-}$ *apoE*$^{+/-}$ double heterozygotes. In the second step, the F_1 generation was intercrossed to generate *apoA-I*$^{-/-}$ *apoE*$^{-/-}$ mice. The *apoE*$^{-/-}$ *apoB*$_{100}$ only and *apoE*$^{-/-}$ *apoB*$_{48}$ only mice were generated by gene-targeting procedures by Farese et al. (*26*) (Gladstone Institute of Cardiovascular Disease, San Francisco, CA) and were in a mixed genetic background (60% B6, 27% FVB/N, 13% 129/Sv). All mice in this study were fed a chow diet. At each step of breeding, pups were screened by PCR of genomic DNA (*19*). A single primer pair was used to screen the *apoE*$^{-/-}$ mice (EKO-F, 5′-GTC TCG GCT CTG AAC TAC ATA G-3′, and EKO-R, 5′-GCA AGA GGT GAT GGT ACT CG-3′), which generated a 600 bp band for the wild-type allele and a 1600 bp band for the targeted allele. The primers used to screen the *apoA-I*$^{-/-}$ mice were mAI-F, 5′-AGG TAA GTG CTG CTA CCT GCC-3′, and mA-R, 5′-GGA CAC ATA GTC TCT GCC GCT-3′, which generated a 500 bp band for the wild-type allele and a 1500 bp band for the targeted allele. The genotype of *apoA-I*$^{-/-}$ *apoE*$^{-/-}$ mice was confirmed by phenotypic analysis of plasma for elevated total cholesterol concentration in the case of the *apoE*$^{-/-}$ genotype and for the absence of mouse apoA-I, using Western blot analysis with anti-mouse apoA-I antibody, in the case of the *apoA-I*$^{-/-}$ genotype. All mice used in this study were at least 24 weeks of age. Whole blood was obtained by cardiac puncture of anesthetized mice (ketamine, 50 mg/kg, and xylazine, 20 mg/kg) after a 4 h fast.

Lipid and Lipoprotein Analysis. Total cholesterol (Roche), free cholesterol (Wako), phospholipid (Wako), and triglyceride (Roche) concentrations in plasma or isolated lipoprotein fractions were determined by enzymatic assay following instructions from the manufacturer.

[2] LpX is defined as an abnormal lipoprotein which is present in large amounts in individuals suffering from obstructive liver diseases. It exists as a bilayer vesicle of equimolar phospholipids and unesterified cholesterol containing small amounts of plasma proteins (mainly albumin) in its internal aqueous compartment together with some apolipoproteins adsorbed on its surface.

Pooled plasma (500 μL) from B6, *apoA-I*$^{-/-}$, *apoE*$^{-/-}$, and *apoA-I*$^{-/-}$ *apoE*$^{-/-}$ mice was subjected to fast protein liquid chromatography (FPLC) fractionation on Superose 6 (1 cm × 30 cm) and Superose 12 (1 cm × 30 cm) columns in series to separate VLDL-, LDL-, and HDL-sized particles. One milliliter of each lipoprotein fraction was subjected to lipid extraction (*27*) with 5α-cholestane added as internal control. The lipid extracts were dried under N_2, dissolved in hexane, and analyzed for FC on a DB 17 gas−liquid chromatography column (*28*). For total cholesterol analysis, the samples were incubated with 1 mL of 100% ethanol and 200 μL of 8.9 N KOH at 60 °C for 1 h. Then cholesterol was extracted by adding 2 mL of hexane and 1 mL of water. After the extract was vortexed and centrifuged, the upper phase (hexane) was transferred to a clean tube and dried, and the lipid extract was dissolved in a small volume of hexane and analyzed for total cholesterol by gas−liquid chromatography. The FC and TC concentrations of VLDL, LDL, and HDL in plasma were calculated as the fractional distribution of FC and TC in each lipoprotein fraction multiplied by the respective concentration in whole plasma.

Endogenous LCAT Assays. Endogenous LCAT cholesterol esterification rate (CER) in whole plasma was measured using a modification of the Stokke and Norum procedure (*29*). A tracer amount of [^{3}H]-cholesterol in acetone was added into a 50 mg/mL bovine serum albumin (BSA) solution, and the acetone was evaporated under N_2. Seventy-five microliters of plasma were incubated with the BSA solution containing 3×10^6 dpm of [^{3}H]-cholesterol on ice overnight to allow the [^{3}H]-cholesterol tracer to equilibrate evenly across the entire spectrum of lipoproteins (similar FC specific activity among lipoproteins was confirmed in pilot studies). The sample was diluted to 300 μL with 0.2 M phosphate buffer (pH 7.4) and divided into three aliquots. Two aliquots were incubated at 37 °C for 30 min as duplicates; the remaining aliquot was maintained at 4 °C, as a control. All subsequent procedures were the same as the exogenous LCAT assay described previously (*30*). Briefly, after incubation, the samples were placed on ice, and lipid was extracted by the Bligh/Dyer method. The extracted lipids were subjected to thin-layer chromatography (TLC) using a neutral solvent system to separate FC and CE radiolabel, which was then quantified by scintillation counting as described previously (*30*). Endogenous LCAT activity was expressed as percentage of FC esterified (calculated as CE/(CE + FC)) and as nanomoles of CE formed per milliliter of plasma (calculated as plasma FC concentration × (%FC esterified/100%)) during the 0.5 h incubation.

Endogenous LCAT CER on apoB LP particles was measured in pooled plasma (4−6 mice) from B6, *apoA-I*$^{-/-}$, *apoE*$^{-/-}$, and *apoA-I*$^{-/-}$ *apoE*$^{-/-}$ mice. Five hundred microliters of pooled plasma from each genotype were fractionated into VLDL-, LDL-, and HDL-sized particles by FPLC, and FC concentration in each fraction was determined by gas−liquid chromatography. Another aliquot (300 μL) of the same plasma pool was incubated with a BSA solution containing [^{3}H]-cholesterol on ice overnight and then split into three aliquots. One aliquot remained on ice and served as control; the other two aliquots were incubated at 37 °C for 1 or 2 h in 0.2 M phosphate buffer. After incubation, all samples were adjusted to 5 mM DTNB (5,5′-dithiobis-2-nitrobenzoic acid) to inhibit LCAT. The samples were injected onto FPLC (Superose 6 and Superose 12 in series) to isolate VLDL, LDL, and HDL fractions, which were then quantified for the amount of radiolabeled FC and CE as described above.

Cloning, Expression, and Purification of Carboxy-Terminal Histidine-6 Tagged Mouse LCAT (mLCATh6). The mLCAT cDNA in pUC13 vector (pUC-mLCAT) was kindly provided by Dr. Jake Lusis, UCLA. The mLCAT cDNA was restricted from pUC13 by *Eco*RI digestion and ligated into the pCMV5 expression vector (pCMV5-mLCAT). A mutagenesis PCR was performed with a 5′ complementary forward primer (5′-TCA GTC CTG GAA GGA CCA CT-3′) and a 3′ reverse primer (5′-GC TCT AGA TTA ATG ATG ATG ATG ATG ATG TTC AGG GGG TGG C-3′) designed to append the sequence for six carboxy-terminal histidine residues, a stop codon, and a 3′ *Xba*I restriction site. The 700 bp PCR product was restricted with *Bgl*II and *Xba*I, and the resulting 415 bp mLCATh6 fragment was ligated into *Bgl*II and *Xba*I digested pCMV5-mLCAT plasmid. To insert an *Eco*RI digestion site downstream of the mLCATh6 cDNA, an oligo linker (5′-CTA GAA GAA TTC TT-3′) was ligated into *Xba*I digested pCMV5-mLCATh6 plasmid. The mLCATh6 cDNA was then isolated from the pCMV5-mLCATh6 plasmid by *Eco*RI digestion and agarose gel purification and ligated into *Eco*RI-digested pIRESneo vector (Clontech). Chinese hamster ovary (CHO) cells were transfected with pIRESneo-mLCATh6 plasmid by FuGENE 6 (Roche) to generate stable CHO cell lines expressing mLCATh6 as described previously (*31*). The procedure for purification of the mLCATh6 was same as that for hLCATh6 (*31*).

Exogenous LCAT Assay. Two types of exogenous LCAT assays were used in this study. One type was performed using recombinant HDL (80:5:1, 1-palmitoyl-2-oleoyl-*sn*-glycero-3-phosphocholine (POPC)/[^{3}H]-cholesterol/apoA-I) as substrate and mouse plasma (5 μL) as enzyme source. The assays were performed with saturating levels of substrate (1.2 μg of cholesterol per reaction) as described previously (*30*). Assay conditions were designed to minimize product inhibition by keeping CE product formation <20%.

Another type of exogenous LCAT assay was performed using similar-sized VLDL and LDL isolated from the plasma of B6, *apoA-I*$^{-/-}$, *apoE*$^{-/-}$, and *apoE*$^{-/-}$ *apoA-I*$^{-/-}$ mice and purified recombinant mouse or human LCAT with a carboxyl-terminal histidine tag as the source of enzyme. Pools of mouse plasma (4−12 mice) from each genotype were made and quantified for FC concentration by enzymatic assay. The pools were then incubated with a 50 mg/mL BSA solution containing sufficient [^{3}H]-cholesterol to radiolabel each plasma pool to a specific activity of 70 000−100 000 dpm/μg FC, based on the FC content of each plasma pool. Radiolabel equilibration was allowed to continue overnight on ice overnight in the presence of 5 mM DTNB to inhibit cholesterol esterification. The radiolabeled lipoproteins in the plasma pools were then fractionated by FPLC as described above. Fractions (5−6) were pooled in the VLDL and LDL size range to minimize size heterogeneity. For LDL-sized particles, 1 μg of FC and 4.6 μg of recombinant mLCATh6 were incubated at 37 °C for 30 min; for VLDL-sized particles, 0.5 μg of FC and 2.3 μg of recombinant mLCATh6 were incubated at 37 °C for 1 h. Incubations were performed in LCAT assay buffer (*30*). For some assays, 0−116 pmol

of purified recombinant human apoE$_3$ (*32*) or purified human apoA-I (*33*) were incubated with VLDL-sized particles (2 μg of FC) from *apoA-I*$^{-/-}$ *apoE*$^{-/-}$ mice in an exogenous LCAT assay buffer mixture at 37 °C for 1 h to allow apolipoprotein binding before recombinant human histidine-tagged LCAT (hLCATh6) (*34*) was added into the mixture for a 1 h incubation at 37 °C. Processing of the incubations to quantify FC and CE radiolabel has been described previously (*30*). To determine the extent of apolipoprotein binding to VLDL during the incubation, the incubation mixture containing 30 pmol of recombinant human apoE$_3$ or purified human plasma apoA-I per microgram of VLDL FC was fractionated by FLPC and the VLDL fraction was pooled for Western blot analysis as described below.

Mass Quantification of Apolipoproteins on Isolated VLDL and LDL Particles. After the [^{3}H]-cholesterol radiolabeled VLDL- and LDL-sized particles were isolated by FPLC, the relative mass of apoA-I, apoE, apoA-IV, and apoB was quantified by Western blot analysis. An equal amount of apoB LPs (0.2 μg of FC) from each genotype was mixed with ^{125}I-radiolabeled BSA loading control, which was radiolabeled by the ICl procedure (*35*). The samples were subjected to protein precipitation using trichloroacetic acid (7.5% final concentration on ice), and the protein pellet was isolated by centrifugation at 18 000 $\times$ *g* for 15 min. The protein pellets were washed with 80% acetone/0.5 M Tris base (pH 8), dissolved in SDS sample buffer, and analyzed in duplicate on 4−20% (3−20% for apoB quantification) SDS polyacrylamide gradient gels (*36*). The proteins were then transferred to a nitrocellulose membrane, and after the ^{125}I-radiolabeled BSA was visualized by phosphorimager analysis, the membrane was blocked and probed with a primary rabbit antibody. The following primary antibodies were used to probe the blots: anti-mouse apoA-I (Biodesign), anti-mouse apoE (Biodesign), anti-rat apoA-IV (provided by Dr. David L. Williams), and anti-mouse apoB$_{48/100}$ (Biodesign). The anti-mouse apoB$_{48/100}$ antibody was generated using mouse B$_{48}$ as antigen; therefore, its reactivity with B$_{48}$ or B$_{100}$ should be similar. The apolipoprotein bands were detected using ^{125}I-radiolabeled goat anti-rabbit antibody (Biodesign) and analyzed using a phosphorimager (Typhoon 8600, Molecular Dynamics).

Immunoprecipitation of LDL-Sized Particles by Rabbit Anti-mouse AI Antibody. An equal amount of LDL (1 μg of FC) from B6, *apoE*$^{-/-}$, and *apoA-I*$^{-/-}$ mice was incubated with rabbit anti-mouse apoA-I antibody (affinity-purified, Biodesign) overnight, and the antibody was pelleted by centrifugation after incubation with protein A agarose. The pellets were boiled in SDS sample buffer, and the supernatants were separated on the 3−20% SDS polyacrylamide gradient gels. The protein bands were transferred to nitrocellulose membranes, which were then exposed to primary goat anti-human apoB antibody, followed by alkaline phosphatase conjugated anti-goat IgG. The protein bands were visualized by enzymatic reaction using 5-bromo-4-chloro-3-indolyl phosphate (BCIP) and nitroblue tetrazolium (NBT) as substrate.

RESULTS

The activation of LCAT by apoE is only about 20% that of apoA-I when assayed on recombinant HDL substrate particles (*20*). Our previous study suggested that apoE may play an important role in the activation of LCAT on apoB lipoproteins because there was a 4-fold greater content of long chain polyunsaturated CEs, products of the LCAT reaction, in *LDLr*$^{-/-}$ mice compared with *apoE*$^{-/-}$ mice, with little difference in the PL fatty acyl substrate pool (*19*). To determine the physiological role of these apolipoproteins on LCAT activation, we performed exogenous and endogenous LCAT assays using plasma from B6, *apoA-I*$^{-/-}$, *apoE*$^{-/-}$, and *apoE*$^{-/-}$ *apoA-I*$^{-/-}$ mice (Figure 1). Exogenous LCAT activity, using plasma as the enzyme source and rHDL as substrate, is highly correlated with plasma LCAT enzyme protein and is used as a surrogate of enzyme concentration in plasma (*37*). Exogenous LCAT activity using plasma from each genotype of mice as enzyme source was 86%, 65%,

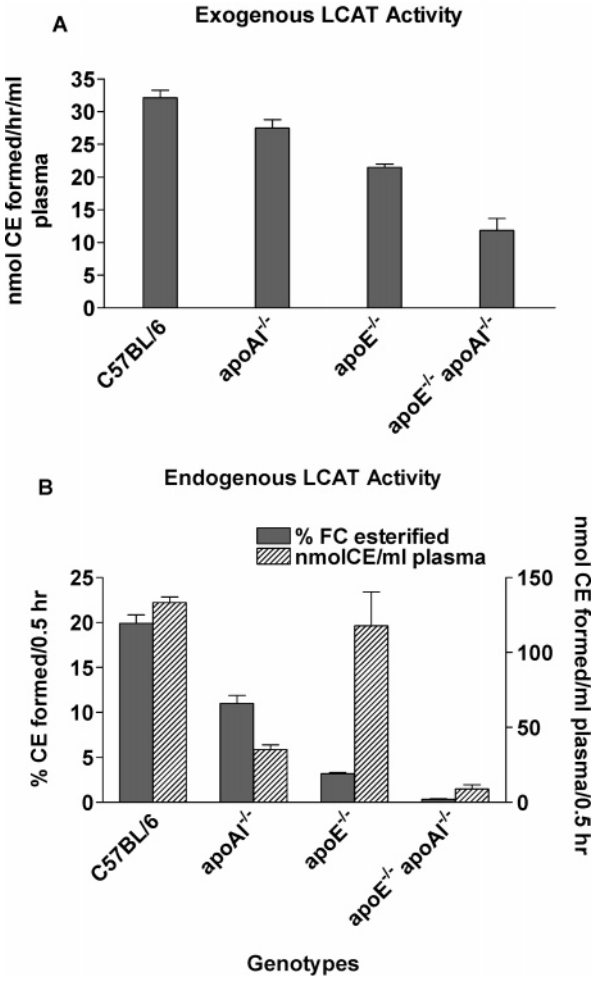

FIGURE 1: Exogenous (panel A) and endogenous (panel B) LCAT assay of whole plasma from chow-fed C57BL/6, *apoA-I*$^{-/-}$, *apoE*$^{-/-}$, and *apoE*$^{-/-}$ *apoA-I*$^{-/-}$ mice. Values are expressed as mean ± SD (n = 3 per group): In panel A, exogenous LCAT activity was measured using whole plasma as LCAT enzyme source and recombinant HDL (rHDL) as substrate. Values are expressed as nmol of cholesterol ester (CE) formed/h/mL of plasma. In panel B, endogenous whole plasma LCAT activities were measured on the same plasma samples used to generate the data in panel A, after incorporation of [^{3}H]-cholesterol. Each plasma sample was assayed in duplicate. Endogenous LCAT cholesterol esterification rate (CER) in whole plasma was expressed as fractional esterification rate (FER) (the percentage of radiolabeled FC esterified during 0.5 h incubation) and molar esterification rate (MER) (nmol of CE formed/mL of plasma during 0.5 h incubation). MER is calculated by multiplying FER by plasma FC concentration.

and 35% that of B6 plasma for *apoA-I*$^{-/-}$, *apoE*$^{-/-}$, and *apoE*$^{-/-}$ *apoA-I*$^{-/-}$ plasma, respectively (Figure 1A). The endogenous LCAT assay measures LCAT cholesterol esterification rate (CER) in whole plasma (Figure 1B), which can be expressed as fractional esterification rate (FER) or molar esterification rate (MER). The FER is the percentage of radiolabeled FC converted to CE in a 30 min incubation, whereas the MER is calculated by multiplying the FER by the plasma FC concentration (Table 1). Both *apoA-I*$^{-/-}$ and *apoE*$^{-/-}$ plasma had reduced FER (mean ± SD; 11.0% ± 1.0% FC esterified and 3.2% ± 0.2% FC esterified, respectively) compared to B6 plasma (19.9% ± 1.0% FC esterified). The FER of *apoE*$^{-/-}$ *apoA-I*$^{-/-}$ plasma (0.32% ± 0.08% FC esterified) was less than 2% that of the B6 mice, and the MER of *apoE*$^{-/-}$ *apoA-I*$^{-/-}$ plasma was reduced to about 7% that of the B6 plasma (8.9 ± 2.7 nmol CE/mL of plasma vs 133.3 ± 3.8 nmol CE/mL of plasma). This dramatic reduction in CER in *apoA-I*$^{-/-}$ *apoE*$^{-/-}$ plasma could not be fully explained by a decrease in plasma LCAT, since the exogenous LCAT activity of *apoA-I*$^{-/-}$ *apoE*$^{-/-}$ plasma remained $^1/_3$ that of B6 plasma (Figure 1A). These combined results indicate that apoE and apoA-I are the only major activators of LCAT in mouse plasma.

The endogenous LCAT CER on apoB LPs was also measured using pooled plasma from B6, *apoA-I*$^{-/-}$, *apoE*$^{-/-}$, and *apoE*$^{-/-}$ *apoA-I*$^{-/-}$ mice (Figure 2). One aliquot of pooled plasma was used to determine the free and esterified cholesterol distribution among the VLDL-, LDL-, and HDL-sized LPs for each genotype (Table 1). After incubation of the plasma pools radiolabeled with [^{3}H]-cholesterol, DTNB was added to stop the LCAT reaction. The LPs were separated by FPLC, extracted by the Bligh−Dyer method, and quantified for the amount of radiolabled FC and CE. In mice lacking apoE, the VLDL and LDL FC concentration in plasma was approximately 100- and 20-fold higher, respectively, than that of mice with apoE (Figure 2A). As shown in Figure 2B,C, greater MER (6.9 nmol CE/mL of plasma/h) and FER (10.6% FC esterified/h) were found for LDL-sized LPs from *apoA-I*$^{-/-}$ mice compared to those from B6 mice control (5.0 nmol CE/mL of plasma/h and 5.9% FC esterified/h, respectively). This suggested that apoA-I might not be the major LCAT activator on apoB LPs in mouse plasma or that the presence of another apolipoprotein, perhaps apoE, could easily compensate for the lack of apoA-I. The FER of LDL from *apoE*$^{-/-}$ mice (0.99% FC esterified/h; Figure 2C) was only $^1/_6$ that of the B6 LDL; however, the MER (16.2 nmol CE/mL of plasma/h; Figure 2B) was around 3 times that of the B6 LDL. This apparent contradiction is explained by the 19-fold higher FC concentration in LDL of *apoE*$^{-/-}$ mice, compared to B6 mice (Figure 2A). Deleting apoA-I from apoE-deficient LDLs (*apoA-I*$^{-/-}$ *apoE*$^{-/-}$) did not lead to a further reduction of FER and led to only a slight decrease in MER (12 vs 16 nmol/(h·mL)). The MER and FER for VLDL showed a similar trend as that for LDL for all the genotypes. The lower FER of apoB LPs in apoE-deficient mice suggested the possibility that apoE serves as an important physiological activator for LCAT cholesterol esterification on apoB LPs.

Interpretation of the endogenous LCAT assay results in whole plasma is confounded by several variables in addition to the presence or absence of different apolipoprotein activators. First, plasma LCAT concentration, estimated by exogenous LCAT assay (Figure 1A), was different among all genotypes. Second, apoE-deficient mice have much higher VLDL and LDL FC concentration than the B6 and *apoA-*

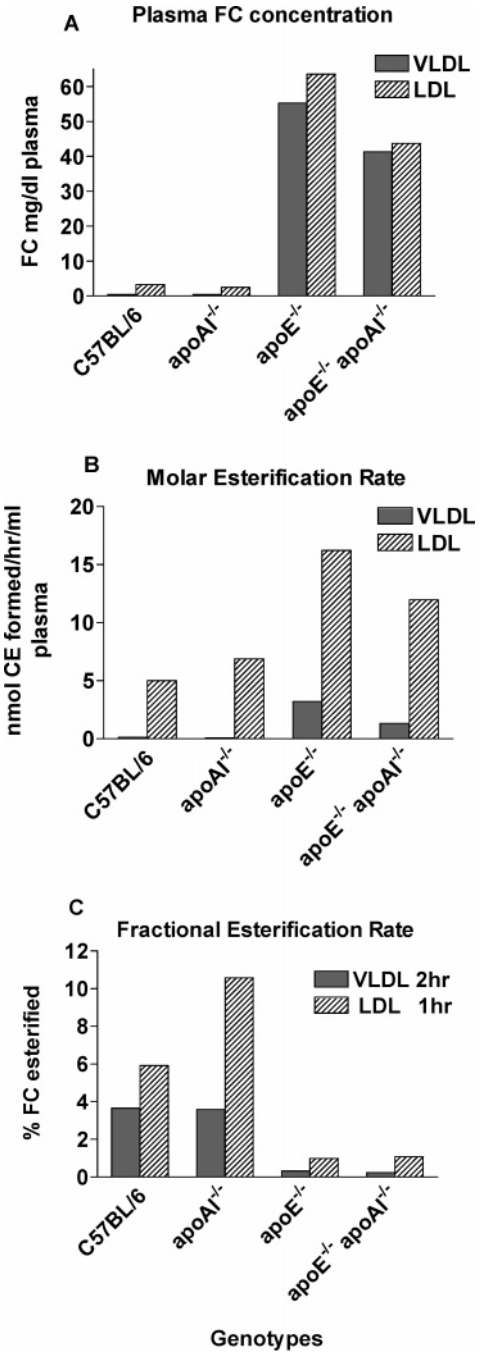

FIGURE 2: Endogenous LCAT cholesterol esterification rate on apoB LPs in plasma of C57BL/6, *apoA-I*$^{-/-}$, *apoE*$^{-/-}$, and *apoE*$^{-/-}$ *apoA-I*$^{-/-}$ mice. In panel A, pooled plasma (500 μL) from each genotype of mice was used to FPLC fractionate lipoproteins and determine FC concentration of VLDL and LDL as described in the Experimental Procedures section. Panel B presents the molar esterification rate of VLDL and LDL in plasma. Whole plasma was radiolabeled with [^{3}H]-cholesterol at 4 °C overnight and then incubated at 37 °C for 1 h. After incubation, VLDL and LDL were fractionated from plasma incubations by FPLC to determine the amount of radiolabeled FC and CE in each lipoprotein fraction. Values are the mean of duplicate assays. Panel C presents the fractional esterification rate of VLDL and LDL in plasma. Same procedure as that in panel B was used, except one plasma sample was incubated for 1 h at 37 °C (LDL) and another was incubated for 2 h (VLDL). Values are the mean of duplicate assays.

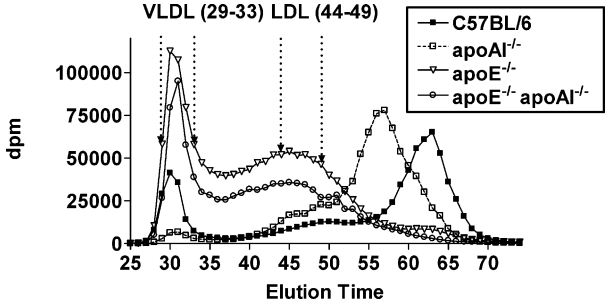

FIGURE 3: Isolation of similar-sized radiolabeled VLDL and LDL particles from mouse plasma. Pooled plasma samples from C57BL/6, *apoA-I*$^{-/-}$, *apoE*$^{-/-}$, and *apoE*$^{-/-}$ *apoA-I*$^{-/-}$ mice were incubated overnight at 4 °C with DTNB (5 mM final concentration) and a BSA solution containing [^{3}H]-cholesterol. The plasma samples were then fractionated by FPLC. The amount of [^{3}H]-cholesterol added to each plasma sample was adjusted to result in similar FC specific activity (70 000−100 000 dpm/μg), based on the assayed FC concentration of each plasma sample. Because of the large differences in FC concentration among the four genotypes (Table 1), different aliquots of individual FPLC fractions were taken for liquid scintillation counting so that the radioactivity elution profile of all four genotypes would be similar in magnitude; thus, in this figure, the radiolabel elution profile is not proportional to FC concentration in plasma. The indicated fractions for VLDL and LDL were pooled for subsequent analysis.

I$^{-/-}$ mice (Figure 2A). Third, the lipid composition and particle size of the apoB LPs may vary among the different genotypes. To control for these confounding variables, we performed exogenous LCAT assays using purified recombinant mLCATh6 and apoB LPs isolated from the plasma of B6, *apoA-I*$^{-/-}$, *apoE*$^{-/-}$, and *apoE*$^{-/-}$ *apoA-I*$^{-/-}$ mice. The apoB LPs, radiolabeled with [^{3}H]-cholesterol, were separated by FPLC, and fractions were pooled over a narrow elution range to minimize size differences of VLDL or LDL among the four genotypes. Figure 3 shows the FPLC column elution of [^{3}H]-cholesterol and the fractions pooled for subsequent analysis. The lipid composition of these LDL and VLDL fractions is shown in Tables 2 and 3, respectively. In general, the lipid compositions of LDLs from different genotypes were similar. The lipid core-to-surface ratio ((TG + CE)/(PL + FC)) was similar for LDLs among the four genotypes, suggesting that LDL particle size was similar among the pooled LDL fractions. The LDLs from *apoE*$^{-/-}$ and *apoE*$^{-/-}$ *apoA-I*$^{-/-}$ mice contained a lower percentage of TG in the core compared to LDLs from B6 and *apoA-I*$^{-/-}$ mice. The esterified cholesterol to total cholesterol ratio (EC/TC) was similar for *apoA-I*$^{-/-}$, *apoE*$^{-/-}$, and *apoE*$^{-/-}$ *apoA-I*$^{-/-}$ mice, but was slightly lower for the B6 mice. The VLDL isolated from *apoE*$^{-/-}$ and *apoE*$^{-/-}$ *apoA-I*$^{-/-}$ mice had EC/TC ratios that were around 2-fold greater than those of B6 and *apoA-I*$^{-/-}$ mice. The major core lipid was CE for VLDL from *apoE*$^{-/-}$ and *apoE*$^{-/-}$ *apoA-I*$^{-/-}$ mice, whereas TG was the major core lipid for VLDL of B6 and *apoA-I*$^{-/-}$ mice. Compared to B6 and *apoA-I*$^{-/-}$ mice, the *apoE*$^{-/-}$ and *apoE*$^{-/-}$ *apoA-I*$^{-/-}$ mice had a higher percentage of surface lipid constituents in VLDL, which resulted in a reduced (TG + CE)/(PL + FC) ratio and suggested a smaller average size for these particles compared to those from B6 and *apoA-I*$^{-/-}$ mice.

The CER of purified recombinant mLCATh6 with LDL (1 μg FC) from each genotype is shown in Figure 4A. The CER of LDL from B6 and *apoA-I*$^{-/-}$ mice was 5.67% ± 0.9% and 6.32% ± 0.11% FC esterified/30 min, respectively; whereas the values for LDL from *apoE*$^{-/-}$ and *apoE*$^{-/-}$ *apoA-I*$^{-/-}$ mice were lower, 1.16% ± 0.1% and 1.07% ± 0.02% FC esterified/30 min, respectively. Compared with LDL from B6 and *apoE*$^{-/-}$ mice, LDLs from *apoA-I*$^{-/-}$ mice contained no apoA-I but were still able to support LCAT-mediated esterification. However, apoE-deficient LDL particles derived from *apoE*$^{-/-}$ and *apoE*$^{-/-}$ *apoA-I*$^{-/-}$ had $^1/_6$ the LCAT reactivity observed with LDL particles from B6 and *apoA-I*$^{-/-}$ mice. Similar results were observed with VLDL-sized particles (Figure 4B), although the CERs were less than those observed with LDL. Our data suggest that apoE might be more important than apoA-I for activation of LCAT on apoB LPs.

Table 1: Cholesterol Concentration of Whole Plasma and Lipoproteins[a]

	C57BL/6				*apoA-I*$^{-/-}$				*apoE*$^{-/-}$				*apoE*$^{-/-}$ *apoA*-I$^{-/-}$			
	plasma	VLDL	LDL	HDL	plasma	VLDL	LDL	HDL	plasma	VLDL	LDL	HDL	plasma	VLDL	LDL	HDL
TC	64.27	0.61	6.97	56.70	30.32	1.02	8.03	21.27	336.62	158.71	155.00	22.91	227.53	120.66	105.51	1.37
FC	17.16	0.45	3.27	13.44	9.79	0.45	2.51	6.83	125.67	55.28	63.55	6.84	85.22	41.28	43.66	0.28
EC	47.11	0.16	3.70	43.26	20.54	0.57	5.52	14.45	210.95	103.43	91.45	16.07	142.31	79.38	61.84	1.09
EC/TC	0.73	0.26	0.53	0.76	0.68	0.56	0.69	0.68	0.63	0.65	0.59	0.70	0.63	0.66	0.59	0.80

[a] Plasma pools were obtained from 4−12 chow-fed mice of the indicated genotypes. Plasma VLDL, LDL, and HDL were isolated by FPLC. The free and esterified cholesterol was measured by GC as described in the Experimental Procedures section. Values are the mean of duplicate determinations and are expressed as mg/dL, except for the EC/TC ratio. TC = total cholesterol; FC = free cholesterol; EC = esterified cholesterol.

Table 2: Lipid Composition of Isolated LDL-Sized Particles[a]

	fractional lipid composition (%)						
genotype	FC	CE	TG	PL	EC/TC	TG/(CE + TG)	(TG + CE)/(PL + FC)
C57Bl/6	13.7	28.9	29.4	28.0	0.557	0.504	1.394
apoA-I$^{-/-}$	12.5	33.2	27.4	27.0	0.614	0.452	1.536
apoE$^{-/-}$	17.9	49.2	6.3	26.6	0.623	0.114	1.249
apoE$^{-/-}$ *apoA-I*$^{-/-}$	18.4	46.4	7.1	28.0	0.602	0.133	1.154

[a] LDL-sized particles were pooled from the FPLC fractions as indicated in Figure 3. Chemical assays were performed by enzymatic assays as described in the Experimental Procedures section. TC = total cholesterol; FC = free cholesterol; EC = esterified cholesterol; TG = triglyceride; PL = phospholipid. Values are the mean of duplicate assays. (TG + CE)/(PL + FC) is an estimate of the core-to-surface ratio, assuming most of the FC is in the surface of LDL.

Table 3: Lipid Composition of Isolated VLDL-Sized Particles[a]

genotype	fractional lipid composition (%) FC	CE	TG	PL	EC/TC	TG/(CE + TG)	(TG + CE)/(PL + FC)
C57BL/6	5.6	2.9	76.4	15.1	0.241	0.963	3.851
apoA-I$^{-/-}$	8.8	5.9	66.5	18.7	0.287	0.918	2.631
apoE$^{-/-}$	17.9	53.7	7.4	20.9	0.643	0.122	1.575
apoE$^{-/-}$ *apoA-I*$^{-/-}$	19.3	52.3	4.5	23.9	0.618	0.080	1.314

[a] VLDL-sized particles were pooled from the FPLC fractions as indicated in Figure 3. Chemical assays were performed by enzymatic assays as described in the Experimental Procedures section. TC = total cholesterol; FC = free cholesterol; EC = esterified cholesterol; TG = triglyceride; PL = phospholipid. Values are the mean of duplicate assays. (TG + CE)/(PL + FC) is an estimate of the core-to-surface ratio, assuming most of the FC is in the surface of LDL.

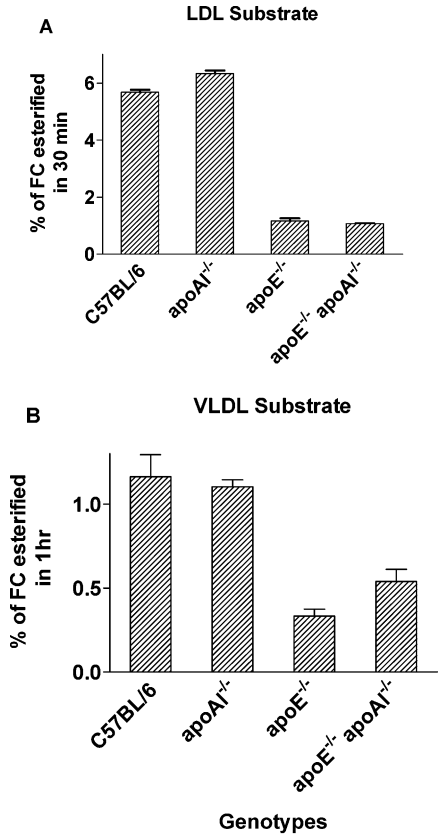

FIGURE 4: Exogenous LCAT assays using isolated VLDL- and LDL-sized particles as substrates. Plasma from the indicated genotypes of mice was radiolabeled with [^{3}H]-cholesterol overnight at 4 °C and then fractionated by FPLC to obtain similar-sized VLDL and LDL particles for all four genotypes of mice (see Figure 3). The VLDL and LDL were then incubated with purified recombinant mLCATh6, and the amount of CE formation was determined. The values represent the mean ± SD of triplicate determinations. In panel A, LDL-sized particles (1 μg FC) were incubated with 4.6 μg of recombinant mLCATh6 at 37 °C for 30 min. In panel B, VLDL-sized particles (0.5 μg FC) were incubated with 2.3 μg of recombinant mLCATh6 at 37 °C for 1 h.

We also compared the relative amount of apolipoproteins on the isolated LDL- (Figure 5) and VLDL-sized LPs (Figure 6) from each genotype using Western blot analysis. As shown in Figures 5D and 6D, the relative amount of apoB on LDL or VLDL particles was similar among all the genotypes. This result indicated that the number of apoB lipoprotein particles and the FC content per particle were similar in the LCAT assays, since substrate addition in assays and sample loading of SDS−PAGE gels was made based on FC content. ApoB$_{100}$ was the dominant apoB form on LDLs from B6 and *apoA-I*$^{-/-}$ mice, whereas apoB$_{48}$ was the dominant apoB form on the LDLs from *apoE*$^{-/-}$ and *apoE*$^{-/-}$ *apoA-I*$^{-/-}$ mice. For VLDL particles, apoB$_{48}$ was the primary apoB form for all the genotypes. Compared to B6 mice, *apoE*$^{-/-}$ mice had a 2-fold increase of apoA-I content on both LDL- and VLDL-sized LPs (Figures 5A and 6A). Despite the increased apoA-I content on VLDL and LDL particles in apoE-deficient mice, it could not compensate for the low LCAT activity associated with apoE-deficient particles (Figure 4). This suggested that apoA-I might not be able to activate LCAT on apoB LPs as efficiently as it does on the HDL and that apoE might be a better activator for LCAT on apoB LPs. The LDLs from *apoA-I*$^{-/-}$ mice contained about 60% of the apoE content of LDLs from B6 mice, whereas apoE content of VLDL-sized LPs was similar between *apoA-I*$^{-/-}$ and B6 mice. The apoA-IV content was low on most of the isolated apoB LPs except the LDLs from *apoE*$^{-/-}$ *apoA-I*$^{-/-}$ mice, which showed an 8-fold increase of apoA-IV content compared to *apoE*$^{-/-}$ LDL. However, the striking increase in apoA-IV in *apoE*$^{-/-}$ *apoA-I*$^{-/-}$ LDL did not result in any detectable increase in LCAT activation (Figure 4A). The enrichment of apoA-IV on VLDL of *apoE*$^{-/-}$ *apoA-I*$^{-/-}$ mice compared with *apoE*$^{-/-}$ mice was less striking (Figure 6C) than that observed for LDL (Figure 5C) but was associated with an increase in LCAT activity (Figure 4B; 0.54% ± 0.07% vs 0.33% ± 0.04% per hour for *apoE*$^{-/-}$ *apoA-I*$^{-/-}$ and *apoE*$^{-/-}$, respectively).

One possibility that we considered was that B$_{100}$ may be an activator of LCAT and its presence on LDL particles in B6 and *apoA-I*$^{-/-}$ mice may explain the higher LCAT reaction rates. To formally test this possibility, we compared the exogenous LCAT activity on isolated LDLs from apoB$_{100}$-only *apoE*$^{-/-}$ mice vs B$_{48}$-only *apoE*$^{-/-}$ mice. In the absence of apoE on apoB LPs, the LDL containing only apoB$_{100}$ had a lower CER (0.95% ± 0.065% FC esterified/30 min) compared to LDL containing only apoB$_{48}$ (1.81% ± 0.024% FC esterified/30 min). Therefore, it seems unlikely that apoB$_{100}$ plays a role in the LCAT activation.

Although the results in Figures 5 and 6 demonstrate the presence of apoA-I and apoE in our isolated VLDL and LDL fractions, the data do not address whether these apolipoproteins are actually bound to apoB-containing particles. Available evidence in the literature supports the presence of apoE on VLDL and LDL particles using immunoaffinity separation techniques (*25*, *38*, *39*). In addition, human LDL incubated with cultured Y1 adrenocortical cells expressing human apoE was shown to contain one molecule of apoE per LDL particle (*40*). However, the presence of apoA-I on LDL particles is less certain. One potential explanation for the better activation of LCAT by apoE compared to apoA-I is that apoE is

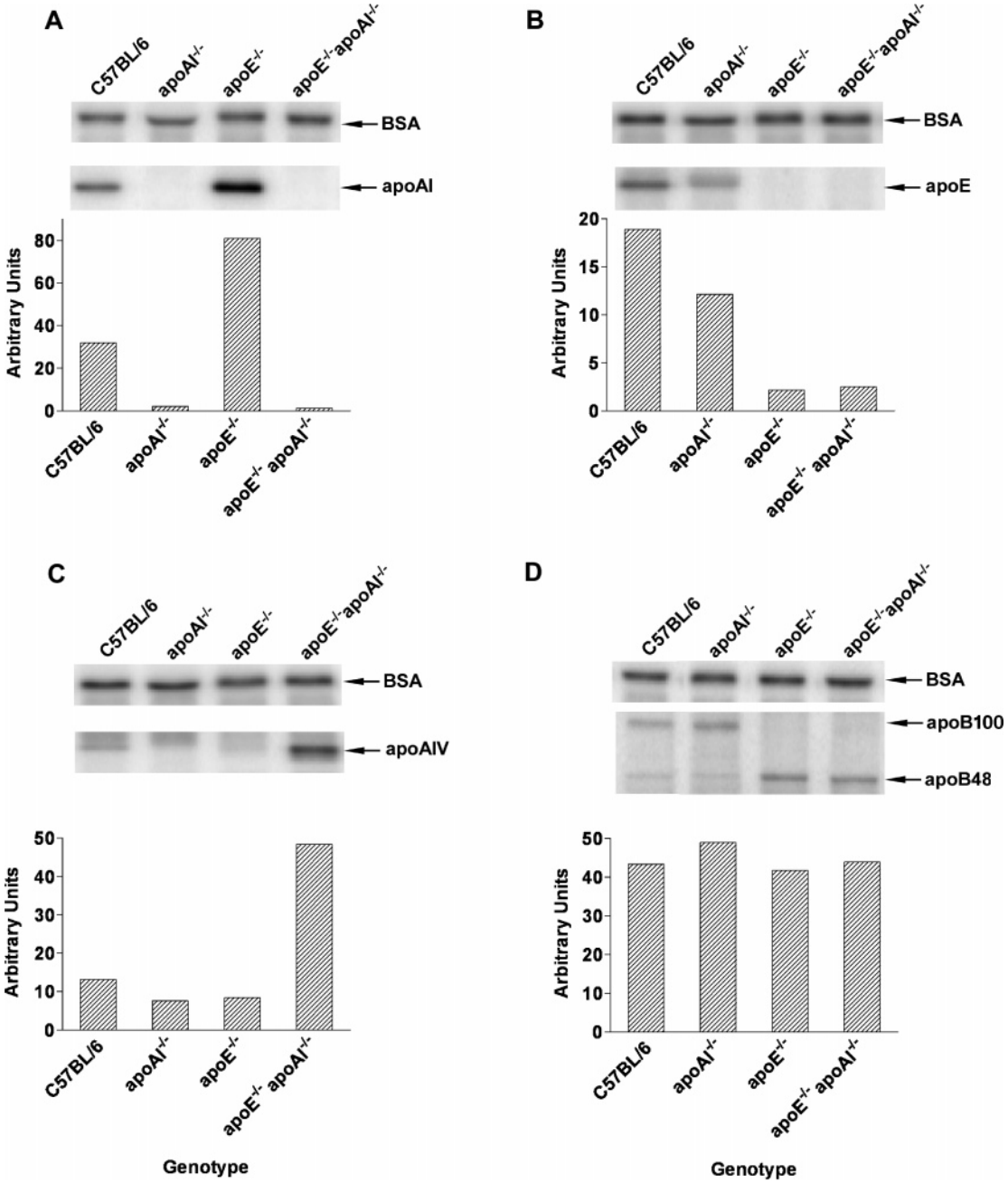

FIGURE 5: Comparison of apolipoproteins on LDL-sized particles from C57BL/6, *apoA-I*$^{-/-}$, *apoE*$^{-/-}$, and *apoE*$^{-/-}$ *apoA-I*$^{-/-}$ mice. An equal amount of LDL FC (0.2 μg) from each genotype was mixed with ^{125}I-labeled BSA loading control; the proteins were precipitated with TCA and then separated on 4−20% SDS polyacrylamide gradient gels. After electrophoresis, the proteins were transferred to nitrocellulose membranes and the ^{125}I-radiolabeled BSA was visualized by phosphorimager analysis. The membrane was then blocked and probed with the primary antibody as described in the Experimental Procedures section. The apolipoprotein bands were detected by ^{125}I-radiolabeled secondary antibody and phosphorimager analysis. The density of each band was quantified as arbitrary units, and the mean density of duplicate blots is plotted. Panel A shows the mouse anti-apoA-I blot, panel B the mouse anti-apoE blot, panel C the mouse anti-apoA-IV blot, and panel D the mouse anti-apoB blot.

associated with LDL particles, whereas apoA-I is on non-LDL particles (i.e., contaminating HDL). To address this issue in our study, we performed immunoprecipitation of our isolated LDL particles with antibody directed against mouse apoA-I, separated the immunoprecipitated proteins by SDS−PAGE, transferred the separated proteins to nitrocellulose membranes and probed the blot with anti-apoB antiserum. As shown in Figure 7, LDL particles isolated from B6 and *apoE*$^{-/-}$ mice were immunoprecipitated with anti-mouse apoA-I antibodies, whereas LDL particles from *apoA-I*$^{-/-}$ mice were not, suggesting that apoA-I was associated with apoB-containing particles in the LDL fraction and would potentially be available to activate LCAT.

To directly test the hypothesis that apoE is a better activator of LCAT than apoA-I on apoB LPs, we added increasing amounts of human apoE$_3$ or human apoA-I to VLDL, isolated from the plasma of *apoE*$^{-/-}$ *apoA-I*$^{-/-}$ mice by FPLC. The samples were incubated for 1 h at 37 °C to allow the added apolipoproteins to bind to the VLDL particles before addition of recombinant hLCATh6; the samples were then incubated at 37 °C for 1 h to allow LCAT-mediated CE formation. The LCAT activity results are shown

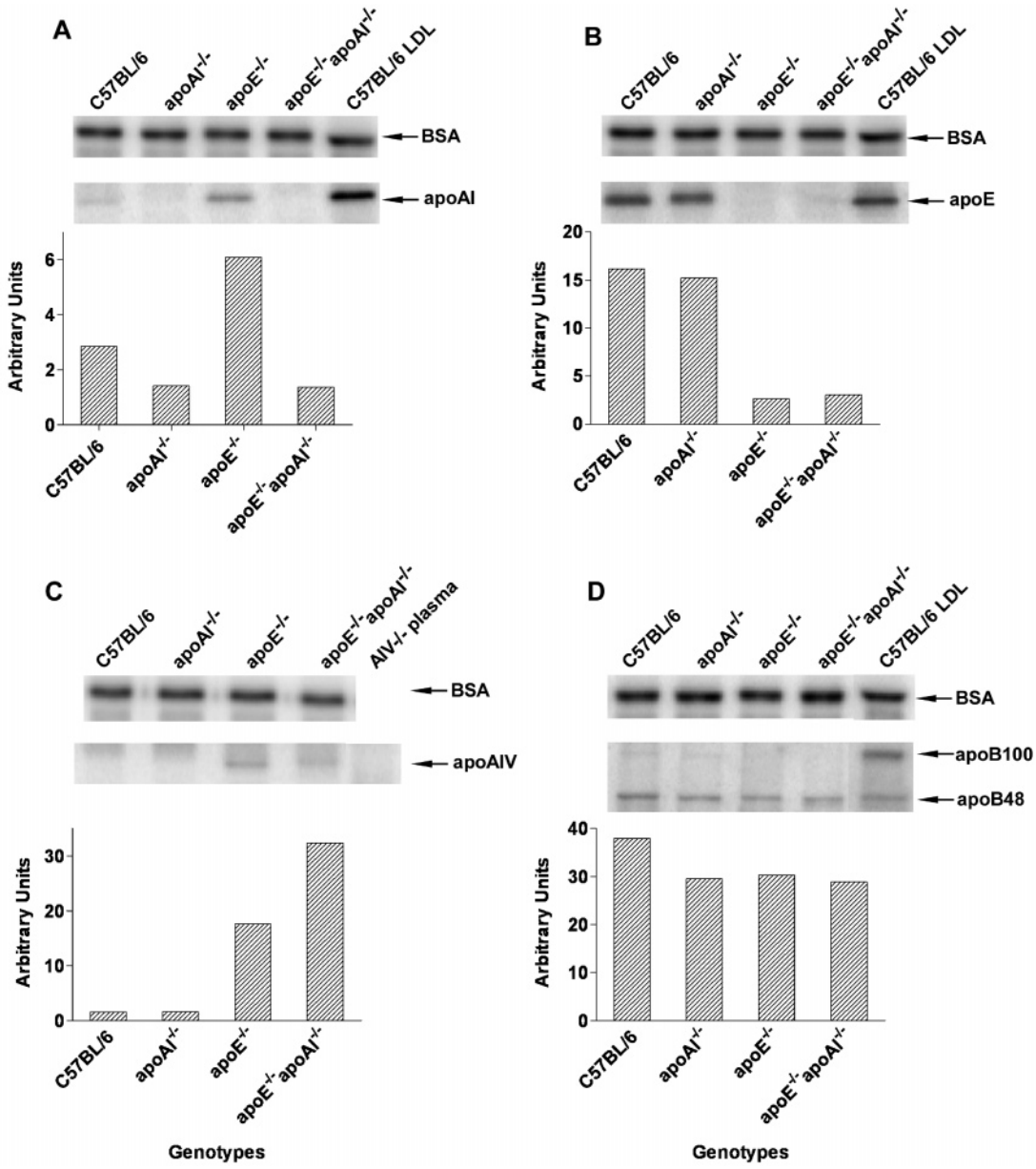

FIGURE 6: Comparison of apolipoproteins on VLDL-sized particles from C57BL/6, *apoA-I*$^{-/-}$, *apoE*$^{-/-}$, and *apoE*$^{-/-}$ *apoA-I*$^{-/-}$ mice. The experimental procedures are the same as those for Figure 5. Panel A shows the mouse anti-apoA-I blot, panel B the mouse anti-apoE blot, panel C the mouse anti-apoA-IV blot, and panel D the mouse anti-apoB blot. A C57Bl/6 LDL sample was added as an additional control in panels A, B, and D; mouse apoA-IV$^{-/-}$ plasma was run as a negative control in panel C.

in Figure 8 as function of the picomoles apolipoprotein per microgram of VLDL FC. The CE formation rate for apoA-I- and apoE-deficient VLDL particles was 0.38% ± 0.026% FC esterified/h. When recombinant human apoE$_3$ was added, the CER was increased by more than 3-fold to 1.32% ± 0.088% FC esterified/h (at 30 pmol of hE3/μg of FC), which was similar to the CER observed with VLDL particles isolated from B6 mice (Figure 4B). However, the increase in cholesterol esterification with equimolar addition of apoA-I was less remarkable and resulted in an 80% increase (0.69% ± 0.04% FC esterified/h) in LCAT activity compared with no apoA-I addition. This difference in cholesterol esterification rate could not be attributed to less apoA-I binding to VLDL compared to apoE because similar amounts of apoE$_3$ (31.2% of total mass) and apoA-I (41.4% of total mass) were found associated with VLDL by Western blot analysis after VLDL particles from the 30 pmol of apolipoprotein/μg of FC incubation were reisolated by FPLC.

DISCUSSION

Previous studies have shown that human LCAT acts directly on apoB LPs to generate CE (*11*, *12*). Studies in mice have also suggested that a significant amount of CE in apoB LPs is the direct product of the LCAT reaction (*19*, *41*). Because LCAT requires activation by an apolipoprotein, the purpose of the present study was to determine which of the several apolipoproteins in apoB LPs was responsible for the activation of LCAT. In exogenous LCAT assays using synthetic HDL substrate particles or vesicles, apoA-I was the most efficient activator, but apoE had 15−40% of the activating potential of apoA-I, depending on the substrate particle (*42*). On the basis of this observation, we hypoth-

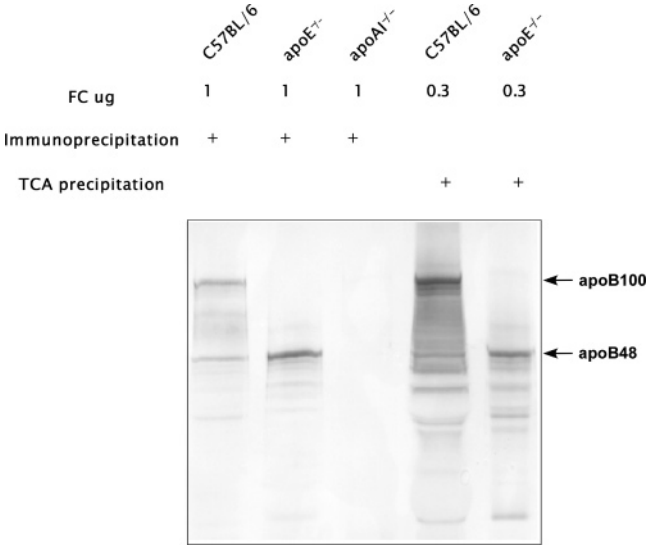

FIGURE 7: Immunoprecipitation of FPLC-isolated LDL particles with rabbit anti-mouse A-I antibody. An equal amount of LDL (1 μg FC) from C57BL/6 (lane 1), *apoE*$^{-/-}$ (lane 2), and *apoA-I*$^{-/-}$ (lane 3) mice was immunoprecipitated with rabbit anti-mouse apoA-I antibody (affinity-purified), and the immunoprecipitated proteins were separated on the 3−20% SDS polyacrylamide gradient gels. TCA-precipitated LDL (0.3 μg FC) from C57BL/6 (lane 4) and *apoE*$^{-/-}$ (lane 5) mice were used as markers for apoB48 and apoB100 migration. The protein bands were transferred to nitrocellulose membranes, which were then exposed to primary goat anti-human apoB antibody, followed by alkaline phosphatase conjugated anti-goat antibody. The protein bands were visualized by enzymatic reaction using BCIP and NBT as substrate.

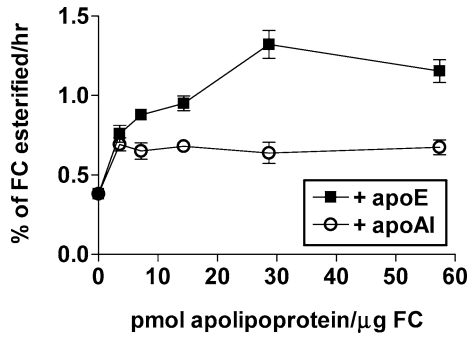

FIGURE 8: Cholesterol esterification rate of human LCAT with VLDL-sized particles from *apoE*$^{-/-}$*apoA-I*$^{-/-}$ mice in the presence of added human E_3 or apoA-I. Increasing amounts of recombinant human E_3 or plasma purified human apoA-I were incubated with VLDL (2 μg FC) at 37 °C for 1 h. Recombinant hLCATh6 was then added to the tubes, the mixtures were incubated at 37 °C for 1 h, and the samples were then processed as described for exogenous LCAT assays in the Experimental Procedures section. The results are expressed as % FC esterified/h and plotted against pmol of apolipoprotein added/μg of VLDL FC. The values are the mean ± SEM of triplicate assays.

esized that apoA-I and apoE may be the major apolipoproteins involved in LCAT activation on apoB LPs. Our experiments resulted in several novel and important findings. First, endogenous LCAT CER was extremely low in the plasma of *apoA-I*$^{-/-}$ *apoE*$^{-/-}$ mice, suggesting that apoA-I and apoE are the only physiological activators of LCAT and that other apolipoproteins in the apoB LP fraction, including apoA-IV, are not as efficient at LCAT activation. Second, apoE deficiency on apoB LPs led to a dramatic reduction of LCAT-mediated esterification, but apoA-I deficient apoB LP particles had LCAT CERs similar to or greater than those for apoB LPs isolated from wild-type mice. Third, adding recombinant human $apoE_3$ to incubations of VLDL from *apoA-I*$^{-/-}$ *apoE*$^{-/-}$ mice and human recombinant LCAT resulted in a 3-fold increase in CE formation, to a level similar to that observed for VLDL from B6 mice, whereas addition of an equimolar amount of human apoA-I resulted in a more modest 80% increase. Thus, on apoB LPs, apoE is a major physiological activator of LCAT and plays a more important role than apoA-I in activating the LCAT reaction.

Two types of assays have been used to measure LCAT activity in our study, exogenous and endogenous. The exogenous assay has been used extensively because it has the advantage of using a uniform substrate, which eliminates some of the variables associated with the endogenous assay, such as substrate concentration, lipid composition, and apolipoprotein composition. Our results were very consistent for both assays in showing that apoE is the preferred activator of LCAT on apoB LPs. The FER of whole plasma (Figure 1B) and apoB LPs isolated from whole plasma (Figure 2B), as well as exogenous assays using isolated VLDL and LDL particles with purified LCAT (Figure 4), all supported the role of apoE in LCAT activation. In addition, add-back experiments demonstrated a greater activation of human LCAT by human $apoE_3$ compared to human apoA-I on VLDL particles (Figure 8). Our experimental data rule out the trivial explanation that apoA-I was not as efficient at activating LCAT on apoB LPs compared to apoE because it could not bind to VLDL and LDL particles. For instance, more apoA-I was found associated with VLDL and LDL particles in *apoE*$^{-/-}$ mice compared to B6 controls (Figures 5 and 6), but apoB LPs from *apoE*$^{-/-}$ mice had low ($\sim^1/_6$ that of B6 mice) LCAT-mediated cholesterol esterification rates (Figure 4). ApoA-I was also found in association with apoB particles in plasma by immunoprecipitation (Figure 7). Finally, human apoA-I added to incubations of VLDL from *apoE*$^{-/-}$ *apoA-I*$^{-/-}$ mice bound as well as equimolar additions of human $apoE_3$ but failed to stimulate human recombinant LCAT esterification to the same extent as $apoE_3$ (Figure 8). These data are consistent with the conclusion that activation of LCAT on apo B LPs was more robust and specific for apoE than for apoA-I.

Based on the whole plasma exogenous and endogenous LCAT assays (Figure 1), apoA-I and apoE are the predominant physiological activators in mouse plasma for LCAT cholesterol esterification. Potentially, apoE and apoA-I may substitute for one another in LCAT activation when either one is missing from plasma as a result of gene targeting or mutations that affect the activation of LCAT. However, deleting apoA-I from apoB LPs (i.e., *apoA-I*$^{-/-}$) did not alter LCAT reactivity (Figures 4−6), whereas deleting apoE from apoB LPs resulted in >2-fold increase of apoA-I content, but this could not rescue LCAT activity. These data indicated that apoA-I is relatively ineffective at activating LCAT on apoB LPs and cannot substitute for apoE in this role. Besides the absence of apoE, the apoB composition was also altered on LDL from *apoE*$^{-/-}$ and *apoE*$^{-/-}$ *apoA-I*$^{-/-}$ mice compared to B6 and *apoA-I*$^{-/-}$ mice. $ApoB_{48}$, which is the primary apoB on VLDL particles in all four genotypes (Figure 6D), became the predominant apoB on LDL particles from *apoE*$^{-/-}$ and *apoE*$^{-/-}$ *apoA-I*$^{-/-}$ mice, rather than B_{100}, which is the predominant form on LDLs from B6 and *apoA-I*$^{-/-}$ mice (Figure 5D). However, apoE-deficient LDL

containing only $apoB_{100}$ had a lower, not higher, CER compared with apoE-deficient LDL containing only $apoB_{48}$, making it unlikely that $apoB_{100}$ plays a role in LCAT activation.

There are several other factors besides apolipoprotein content that could influence LCAT CER on apoB LPs. These include (1) lipoprotein particle size, (2) PL fatty acid composition, (3) sphingomyelin content, and (4) core lipid content. We isolated VLDL and LDL particles of similar size by FPLC from the study mice to perform exogenous LCAT assays and showed that the activation differential between apoA-I and apoE was retained with particles of similar size (Figure 4). The similarity in core to surface lipid ratio of isolated LDL particles (Table 2) suggests that our separation procedure did result in similar size particles. The ratio was more variable in VLDL particles, likely reflecting the diminished resolving power of the FPLC column near the void volume. Previous studies have shown that LCAT activity is affected by the fatty acyl composition of the PL substrate pool in LP particles. However, we have shown in a prior study that plasma apoB LP PL fatty acid composition is similar for B6 and *apoE*$^{-/-}$ mice (*19*) and cannot explain the marked difference in LCAT-mediated cholesterol esterification of apoB LP particles isolated from these two mouse strains (Figure 4). We also found that LDL PL fatty acid composition was similar among all four genotypes in this study (data not shown). The phospholipid headgroup can also affect LCAT activity. Sphingomyelin (SPM) has been shown to inhibit LCAT activity in recombinant HDL (*43*) and LDL particles (*44*). Subbaiah and Liu (*45*) reported that after a 5-fold enrichment of HDL_3 with SPM (SPM/PC ratio 0.14 to 0.73), LCAT activity was inhibited by 50%. LDL from *apoE*$^{-/-}$ mice have a 2-fold enrichment in SPM (0.36) compared with B6 mice (0.18) (*46*). Therefore, the magnitude of SPM enrichment in apoB LPs of *apoE*$^{-/-}$ and *apoE*$^{-/-}$ *apoA-I*$^{-/-}$ mice could not explain the marked decrease in LCAT activity of VLDL and LDL particles in our study (Figure 4). Another possible explanation for divergent LCAT activities for apoB LPs among the four genotypes of mice could be due to differences in particle core composition. An enrichment in LP core CE content has been reported to result in product feedback inhibition of the enzyme (*47*). However, the similar LDL EC/TC ratios among the four genotypes of mice makes this explanation unlikely (Table 2). Spherical synthetic HDL containing increased TG content relative to CE showed reduced activity with LCAT regardless of the size or relative content of the substrate particles (*48*). Thus, the reduced amount of TG core lipid in the apoB LPs from *apoE*$^{-/-}$ and *apoE*$^{-/-}$ *apoA-I*$^{-/-}$ mice should not result in a decreased LCAT CER in these particles. In summary, we believe that the reduced apoE content of LDL particles from *apoE*$^{-/-}$ and *apoE*$^{-/-}$ *apoA-I*$^{-/-}$ mice is responsible for the low LCAT CER compared LDLs from B6 and *apoA-I*$^{-/-}$ mice.

ApoE is only 17−18% as effective as apoA-I at activating LCAT on synthetic discoidal HDL particles; however, on larger apoB LP particles with a lipid core, our data demonstrate that apoE is more effective than apoA-I in LCAT activation. The molecular explanation for this change in activation potential is unknown but may be related to the apolipoprotein conformation differences between small discoidal HDL and large spherical particles. Several studies have demonstrated that size, shape (sphere or disk), and the core lipid content of the synthetic HDL particles affects the secondary structure and net surface charge of apoA-I on lipoprotein particles (*49*, *50*). On discoidal HDL without a neutral lipid core or small spherical HDL with a small lipid core, the conformation of apoA-I appears favorable for LCAT activation. However, on larger LP particles, such as LDL, with a larger neutral lipid core, the folding and organization of apoA-I may preclude its activation of LCAT, whereas the conformation of apoE may be more favorable for activation.

Activation of LCAT by apolipoproteins may involve protein−protein interactions that lead to increased activity, or alternatively, the apolipoprotein may help present monomeric substrate molecules from the surface of lipoprotein particles to the active site of the enzyme. If LCAT activation occurs by direct contact with apolipoproteins, our data are compatible with the hypothesis that apoA-I and apoE bind to different regions of LCAT, based on the activity profile of FED patients. FED patients have normal LCAT activity on LDL particles, but no activity on HDL particles. Based on our findings, we speculate that FED LCAT has a defect in interacting with apoA-I, but not apoE. As a result, apoA-I would not activate LCAT on HDL nor LDL; however, esterification activity would be maintained on LDL through activation by apoE. Peelman et al. (*51*), using a molecular model of LCAT based on structural homology with lipases, propose that most mutations in FED are localized on the outer hydrophilic surface of the amphipathic helical segments, which they hypothesize may be involved in the interaction with apoA-I. This interaction may be disrupted in FED, but the binding of apoE to a different region of LCAT may be preserved, resulting in enzyme activation.

HDL concentrations were reduced to 40% of normal in *apoA-I*$^{-/-}$ and *apoE*$^{-/-}$ mice compared to B6 controls, but HDL concentrations in *apoE*$^{-/-}$ *apoA-I*$^{-/-}$ mice were 2% of normal (Table 1). Thorngate et al. (*52*) recently reported that lipid-poor apoA-IV (in the HDL fraction) is the primary acceptor for the increased ABCA1-mediated FC efflux in *apoE*$^{-/-}$ *apoA-I*$^{-/-}$ mouse serum, in which apoB LPs had been removed by poly(ethylene glycol) precipitation. However, we could not detect any cholesterol esterification in the HDL fraction of *apoE*$^{-/-}$ *apoA-I*$^{-/-}$ mice (data not shown), suggesting that no other apolipoproteins could substitute for apoA-I or apoE activation of LCAT in the HDL fraction. Although apoA-IV has been shown to activate LCAT on the synthetic substrate particles (*53*), our data indicated that apoB LP particles containing apoA-IV from *apoE*$^{-/-}$ *apoA-I*$^{-/-}$ mice did not stimulate LCAT esterification in LDL particles (Figure 4A) or modestly stimulated esterification in VLDL particles (Figure 4B) compared to particles containing apoE, even though there was a large increase in apoA-IV mass on apoB LPs (Figures 5C and 6C) of *apoE*$^{-/-}$ *apoA-I*$^{-/-}$ mice. Mouse apoA-I and apoE bound to apoB LPs might share some similarities in the tertiary structure, different from apoA-IV and other exchangeable apolipoproteins, which contribute to LCAT activation in this LP fraction.

ACKNOWLEDGMENT

The authors gratefully acknowledge Dr. Aldons (Jake) Lusis for providing us with the mouse LCAT cDNA for these

studies. This paper is dedicated to the memory of Dr. David L. Williams.

REFERENCES

1. Buhman, K. F., Accad, M., and Farese, R. V. (2000) Mammalian acyl-CoA:cholesterol acyltransferases, *Biochim. Biophys. Acta 1529*, 142−154.
2. Rudel, L. L., Lee, R. G., and Cockman, T. L. (2001) Acyl coenzyme A: cholesterol acyltransferase types 1 and 2: structure and function in atherosclerosis, *Curr. Opin. Lipidol. 12*, 121−127.
3. Jonas, A. (2000) Lecithin cholesterol acyltransferase, *Biochim. Biophys. Acta 1529*, 245−256.
4. Glomset, J. A. (1968) The plasma lecithin:cholesterol acyltransferase reaction, *J. Lipid Res. 9*, 155−167.
5. Liu, M., Bagdade, J. D., and Subbaiah, P. V. (1995) Specificity of lecithin:cholesterol acyltransferase and atherogenic risk: Comparative studies on the plasma composition and in vitro synthesis of cholesteryl esters in 14 vertebrate species, *J. Lipid Res. 36*, 1813−1824.
6. Subbaiah, P. V., Liu, M., and Paltauf, F. (1994) Role of *sn*−2 acyl group of phosphatidylcholine in determining the positional specificity of lecithin−cholesterol acyltransferase, *Biochemistry 33*, 13259−13266.
7. Fielding, C. J., Shore, V. G., and Fielding, P. E. (1972) A protein cofactor of lecithin:cholesterol acyltransferase, *Biochem. Biophys. Res. Commun. 46*, 1493−1498.
8. Chen, C. H., and Albers, J. J. (1982) Distribution of lecithin-cholesterol acyltransferase (LCAT) in human plasma lipoprotein fractions. Evidence for the association of active LCAT with low-density lipoproteins, *Biochem. Biophys. Res Commun. 107*, 1091−1096.
9. Barter, P. J. (1983) Evidence that lecithin:cholesterol acyltransferase acts on both high- density and low-density lipoproteins, *Biochim. Biophys. Acta 751*, 261−270.
10. Barter, P. J., Hopkins, G. J., and Gorjatschko, L. (1984) Comparison of human plasma low- and high-density lipoproteins as substrates for lecithin: cholesterol acyltransferase, *Biochim. Biophys. Acta 792*, 1−5.
11. Rajaram, O. V., and Barter, P. J. (1985) Reactivity of human lipoproteins with purified lecithin: cholesterol acyltransferase during incubations in vitro, *Biochim. Biophys. Acta 835*, 41−49.
12. Carlson, L. A., and Holmquist, L. (1985) Evidence for the presence in human plasma of lecithin: cholesterol acyltransferase activity (beta-LCAT) specifically esterifying free cholesterol of combined pre-beta- and beta-lipoproteins. Studies of fish eye disease patients and control subjects, *Acta Med. Scand. 218*, 197−205.
13. Carlson, L. A., and Holmquist, L. (1985) Evidence for deficiency of high-density lipoprotein lecithin: cholesterol acyltransferase activity (alpha-LCAT) in fish eye disease, *Acta Med. Scand. 218*, 189−196.
14. Glomset, J. A., Norum, K. R., and King, W. (1970) Plasma lipoproteins in familial lecithin: cholesterol acyltransferase deficiency: lipid composition and reactivity in vitro, *J. Clin. Invest. 49*, 1827−1837.
15. Norum, K. R., Glomset, J. A., Nichols, A. V., and Forte, T. (1971) Plasma lipoproteins in familial lecithin: cholesterol acyltransferase deficiency: physical and chemical studies of low and high-density lipoproteins, *J. Clin. Invest. 50*, 1131−1140.
16. Forte, T. M., and Carlson, L. A. (1984) Electron microscopic structure of serum lipoproteins from patients with fish eye disease, *Arteriosclerosis 4*, 130−137.
17. Glomset, J. A., Nichols, A. V., Norum, K. R., King, W., and Forte, T. (1973) Plasma lipoproteins in familial lecithin: cholesterol acyltransferase deficiency. Further studies of very low and low-density lipoprotein abnormalities, *J. Clin. Invest. 52*, 1078−1092.
18. Norum, K. R., Glomset, J. A., Nichols, A. V., Forte, T., Albers, J. J., King, W. C., Mitchell, C. D., Applegate, K. R., Gong, E. L., Cabana, V., and Gjone, E. (1975) Plasma lipoproteins in familial lecithin: cholesterol acyltransferase deficiency: effects of incubation with lecithin: cholesterol acyltransferase in vitro, *Scand. J. Clin. Lab. Invest. 35* (Suppl 142), 31−55.
19. Furbee, J. W., Jr., Francone, O. L., and Parks, J. S. (2002) In vivo contribution of lecithin:cholesterol acyltransferase (LCAT) to apolipoprotein B lipoprotein cholesteryl esters in low-density lipoprotein receptor and apolipoprotein E knockout mice, *J. Lipid Res. 43*, 428−437.
20. Jonas, A. (1991) Lecithin-cholesterol acyltransferase in the metabolism of high-density lipoproteins, *Biochim. Biophys. Acta 1084*, 205−220.
21. Cheung, M. C., Wang, D. B., Lum, K. D., and Albers, J. J. (1988) Cholesterol esterification by lecithin-cholesterol acyltransferase in A-I-free plasma, *Biochim. Biophys. Acta 962*, 258−264.
22. Parks, J. S., Li, H., Gebre, A. K., Smith, T. L., and Maeda, N. (1995) Effect of apolipoprotein A-I deficiency on lecithin: cholesterol acyltransferase activation in mouse plasma, *J. Lipid Res. 36*, 349−355.
23. Zorich, N., Jonas, A., and Pownall, H. J. (1985) Activation of lecithin cholesterol acyltransferase by human apolipoprotein E in discoidal complexes with lipids, *J. Biol. Chem. 260*, 8831−8837.
24. Alaupovic, P. (2003) The Concept of Apolipoprotein-defined Lipoprotein Families and Its Clinical Significance, *Curr. Atheroscler. Rep. 5*, 459−467.
25. Koren, E., Alaupovic, P., Lee, D. M., Dashti, N., Kloer, H. U., and Wen, G. (1987) Selective isolation of human plasma low-density lipoprotein particles containing apolipoproteins B and E by use of a monoclonal antibody to apolipoprotein B, *Biochemistry 26*, 2734−2740.
26. Farese, R. V., Jr., Veniant, M. M., Cham, C. M., Flynn, L. M., Pierotti, V., Loring, J. F., Traber, M., Ruland, S., Stokowski, R. S., Huszar, D., and Young, S. G. (1996) Phenotypic analysis of mice expressing exclusively apolipoprotein B48 or apolipoprotein B100, *Proc. Natl. Acad. Sci. U.S.A. 93*, 6393−6398.
27. Bligh, E. G., and Dyer, W. J. (1959) A rapid method of total lipid extraction and purification, *Can. J. Med. Sci. 37*, 911−917.
28. Rudel, L. L., Kelley, K., Sawyer, J. K., Shah, R., and Wilson, M. D. (1998) Dietary monounsaturated fatty acids promote aortic atherosclerosis in LDL receptor-null, human ApoB100-overexpressing transgenic mice, *Arterioscler. Thromb. Vasc. Biol. 18*, 1818−1827.
29. Stokke, K. T., and Norum, K. R. (1971) Determination of lecithin: cholesterol acyltransfer in human blood plasma, *Scand. J. Clin. Lab. Invest. 27*, 21−27.
30. Parks, J. S., Gebre, A. K., and Furbee, J. W. (1999) Lecithin-cholesterol acyltransferase. Assay of cholesterol esterification and phospholipase A2 activities, *Methods Mol. Biol. 109*, 123−131.
31. Zhao, Y., Wang, J., Gebre, A. K., Chisholm, J. W., and Parks, J. S. (2003) Negative charge at amino acid 149 is the molecular determinant for substrate specificity of lecithin: cholesterol acyltransferase for phosphatidylcholine containing 20-carbon sn-2 fatty acyl chains, *Biochemistry 42*, 13941−13949.
32. Morrow, J. A., Arnold, K. S., and Weisgraber, K. H. (1999) Functional Characterization of Apolipoprotein E Isoforms Overexpressed in *Escherichia coli*, *Protein Expression Purif. 16*, 224−230.
33. Nichols, A. V., Gong, E. L., Blanche, P. J., Forte, T. M., and Anderson, D. W. (1976) Effects of guanidine hydrochloride on human plasma high-density lipoproteins, *Biochim. Biophys. Acta 446*, 226−239.
34. Chisholm, J. W., Gebre, A. K., and Parks, J. S. (1999) Characterization of C-terminal histidine tagged human recombinant lecithin:cholesterol acyltransferase, *J. Lipid Res. 40*, 1512−1519.
35. Parks, J. S., and Rudel, L. L. (1982) Different kinetic fates of apolipoproteins A−I and A-II from lymph chylomicra of non-human primates. Effect of saturated versus polyunsaturated dietary fat, *J. Lipid Res. 23*, 410−421.
36. Furbee, J. W., Jr., Sawyer, J. K., and Parks, J. S. (2002) Lecithin: cholesterol acyltransferase deficiency increases atherosclerosis in the low-density lipoprotein receptor and apolipoprotein E knockout mice, *J. Biol. Chem. 277*, 3511−3519.
37. Albers, J. J., Chen, C. H., and Adolphson, J. L. (1981) Lecithin: cholesterol acyltransferase (LCAT) mass; its relationship to LCAT activity and cholesterol esterification rate, *J. Lipid Res. 22*, 1206−1213.
38. Lee, D. M., and Alaupovic, P. (1986) Apolipoproteins B, C-III and E in two major subpopulations of low-density lipoproteins, *Biochim. Biophys. Acta 879*, 126−133.
39. Mahley, R. W. (1988) Apolipoprotein E: cholesterol transport protein with expanding role in cell biology, *Science 240*, 622−630.
40. Swarnakar, S., Reyland, M. E., Deng, J., Azhar, S., and Williams, D. L. (1998) Selective Uptake of Low-Density Lipoprotein-Cholesteryl Ester Is Enhanced by Inducible Apolipoprotein E Expression in Cultured Mouse Adrenocortical Cells, *J. Biol. Chem. 273*, 12140−12147.

41. Lee, R. G., Kelly, K. K., Sawyer, J. K., Farese, R. V., Jr., Parks, J. S., and Rudel, L. L. (2004) Plasma cholesteryl esters provided by lecithin:cholesterol acyltransferase and acyl-coenzyme A:cholesterol acyltransferase 2 have opposite atherosclerotic potential, *Circ. Res. 95*, 988−1004.
42. Jonas, A. (2000) Lecithin cholesterol acyltransferase, *Biochim. Biophys. Acta 1529*, 245−256.
43. Reichl, D., and Sterchi, J. M. (1992) Human peripheral lymph lipoproteins are enriched in sphingomyelin, *Biochim. Biophys. Acta Lipids Lipid Metab. 1127*, 28−32.
44. Liu, M., Krul, E. S., and Subbaiah, P. V. (1992) Effect of apoprotein B conformation on the activation of lysolecithin acyltransferase and lecithin: cholesterol acyltransferase. Studies with subfractions of low-density lipoproteins, *J. Biol. Chem. 267*, 5139−5147.
45. Subbaiah, P. V., and Liu, M. (1993) Role of sphingomyelin in the regulation of cholesterol esterification in the plasma lipoproteins. Inhibition of lecithin-cholesterol acyltransferase reaction, *J. Biol. Chem. 268*, 20156−20163.
46. Jeong, T. S., Schissel, S. L., Tabas, I., Pownall, H. J., Tall, A. R., and Jiang, X. C. (1998) Increased sphingomyelin content of plasma lipoproteins in apolipoprotein E knockout mice reflects combined production and catabolic defects and enhances reactivity with mammalian sphingomyelinase, *J. Clin. Invest. 101*, 905−912.
47. Chajek, T., Aron, L., and Fielding, C. J. (1980) Interaction of lecithin:cholesterol acyltransferase and cholesteryl ester transfer protein in the transport of cholesteryl ester into sphingomyelin liposomes, *Biochemistry 19*, 3673−3677.
48. Sparks, D. L., and Pritchard, P. H. (1989) The neutral lipid composition and size of recombinant high-density lipoproteins regulates lecithin:cholesterol acyltransferase activity, *Biochem. Cell Biol. 67*, 358−364.
49. Wald, J. H., Krul, E. S., and Jonas, A. (1990) Structure of apolipoprotein A−I in three homogeneous, reconstituted high-density lipoprotein particles, *J Biol. Chem. 265*, 20037−20043.
50. Sparks, D. L., Davidson, W. S., Lund-Katz, S., and Phillips, M. C. (1995) Effects of the neutral lipid content of high-density lipoprotein on apolipoprotein A−I structure and particle stability, *J. Biol. Chem. 270*, 26910−26917.
51. Peelman, F., Verschelde, J. L., Vanloo, B., Ampe, C., Labeur, C., Tavernier, J., Vandekerckhove, J., and Rosseneu, M. (1999) Effects of natural mutations in lecithin:cholesterol acyltransferase on the enzyme structure and activity, *J. Lipid Res. 40*, 59−69.
52. Thorngate, F. E., Yancey, P. G., Kellner-Weibel, G., Rudel, L. L., Rothblat, G. H., and Williams, D. L. (2003) Testing the role of apoA-I, HDL, and cholesterol efflux in the atheroprotective action of low-level apoE expression, *J. Lipid Res. 44*, 2331−2338.
53. Steinmetz, A., and Utermann, G. (1985) Activation of lecithin: cholesterol acyltransferase by human apolipoprotein A-IV, *J. Biol. Chem. 260*, 2258−2264.

BI0481489